The Third Pillar of Causal Analysis? A Measurement Perspective on Causal Representations

Dingling Yao [*1] **Shimeng Huang** [*1] **Riccardo Cadei** [1] **Kun Zhang** [2 3] **Francesco Locatello** [1]

Abstract

Causal reasoning and discovery, two fundamental tasks of causal analysis, often face challenges in applications due to the complexity, noisiness, and high-dimensionality of real-world data. Despite recent progress in identifying latent causal structures using causal representation learning (CRL), what makes learned representations useful for causal downstream tasks and how to evaluate them are still not well understood. In this paper, we reinterpret CRL using a measurement model framework, where the learned representations are viewed as proxy measurements of the latent causal variables. Our approach clarifies the conditions under which learned representations support downstream causal reasoning and provides a principled basis for quantitatively assessing the quality of representations using a new Test-based Measurement EXclusivity (T-MEX) score. We validate T-MEX across diverse causal inference scenarios, including numerical simulations and real-world ecological video analysis, demonstrating that the proposed framework and corresponding score effectively assess the identification of learned representations and their usefulness for causal downstream tasks.

1. Introduction

Causal analysis rests on two foundational pillars: causal reasoning and causal discovery. Causal reasoning operates under the assumption that the causal structure is known or can be assumed, and leverages data to make quantitative causal statements, for example, about the average effect of one variable on another. As causal structures are often unknown, causal discovery aims to uncover this structure, assuming that the causal variables of interest are readily observed. In many real-world settings, however, the causal variables may not be directly observable. While originally formulated mostly to enable causal capabilities in machine learning models, Causal Representation Learning (CRL, Schölkopf et al., 2021) has the potential to serve as a third pillar of causal analysis: enabling applications of causality involving unstructured data. For this, we reinterpret causal representation learning using the formalism of "*measurement models*" (Silva et al., 2006), wherein the learned representations serve as proxy measurements for latent causal variables. This perspective of CRL allows us to better characterize when a representation supports downstream causal reasoning, and it also provides a principled basis for quantitatively evaluating the quality of identification.

Methodologically, CRL tackles a more challenging task compared to independent component analysis (ICA) and disentanglement, where the latent variables are assumed to be independent of each other (Hyvärinen and Pajunen, 1999; Hyvarinen et al., 2019; Higgins et al., 2017; Locatello et al., 2019). Instead, CRL aims to unmix a set of causally related latent variables. Many recent causal representation learning works have provided different theoretical results for causal variable identification compiling various problem settings (von Kügelgen et al., 2021; 2024; Zhang et al., 2024b; Ahuja et al., 2024; 2022; Varici et al., 2024; Zhang et al., 2024a; Yao et al., 2024b; Kong et al., 2022; Lippe et al., 2022b; Xie et al., 2024; Dong et al., 2024; Lachapelle et al., 2022; 2023; Yao et al., 2022; Zhang et al., 2024a; Squires et al., 2023; Buchholz et al., 2024; Kong et al., 2023), recently unified by (Yao et al., 2025) into a single general methodology. Although most of the results have been theoretical in nature, machine learning models explicitly empowered with identified causal structure have been shown to be more robust under distributional shifts and provide better out-of-distribution generalization (Fumero et al., 2024; Ahuja et al., 2021; Bareinboim and Pearl, 2016; Zhang et al., 2020; Rojas-Carulla et al., 2018). From an AI for science perspective, CRL has shown its potential in understanding climate physics from raw measurement data (Yao et al., 2024a), answering causal questions in the scope of ecology experiments (Cadei et al.,

[*]Equal contribution [1]Institute of Science and Technology Austria [2]Carnegie Mellon University [3]Mohamed bin Zayed University of Artificial Intelligence (MBZUAI). Correspondence to: Dingling Yao <dingling.yao@ista.ac.at>, Shimeng Huang <shimeng.huang@ista.ac.at>.

SIM Workshop at the 42^{nd} International Conference on Machine Learning, Vancouver, Canada. PMLR 267, 2025.

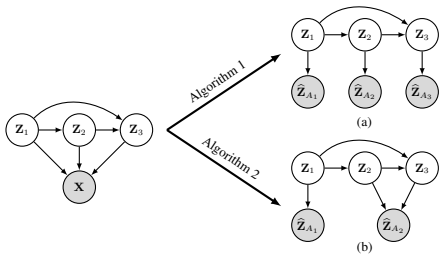

Figure 1: (*Left*) A measurement model where $\mathbf{X}$ is a fully mixed measurement of the causal variables. $\mathbf{X}$ is often termed the *observables* in CRL literature, representing the observed data. (*Right*) Two measurement models specified by different CRL identification algorithms: (a) Algorithm 1 guarantees one-to-one correspondence between the learned representation and causal variables; (b) Algorithm 2 guarantees that $\widehat{\mathbf{Z}}_{A_1}$ corresponds to $\mathbf{Z}_1$ while $\widehat{\mathbf{Z}}_{A_2}$ represents a mixing of $\mathbf{Z}_2$ and $\mathbf{Z}_3$.

2024; 2025; Yao et al., 2025), psychometric studies (Dong et al., 2024), and countless more applications related to biomedicine (Zhang et al., 2024a; Sun et al., 2025; Ravuri et al., 2025; Jain et al., 2024).

Despite recent progress in identifying latent causal structures within causal representation learning, it remains unclear what makes learned representations useful for downstream causal tasks and how to best evaluate them. Building on the proposed measurement model framework, we introduce a new evaluation metric, the Test-based Measurement EXclusivity (T-MEX) Score, which effectively quantifies how well the learned representation aligns with the underlying measurement model. This underlying measurement model can be specified by, for instance, identifiability theory of a CRL algorithm (Fig. 1), assumptions for a particular causal reasoning task (Figs. 4 and 5), or ground truth knowledge. In contrast to commonly used CRL evaluation metrics, which suffer from clear limitations (App. D), we demonstrate that T-MEX reliably assesses both the identifiability (Defn. B.1) and causal validity (Defn. 2.2) of learned representations, as shown in a wide range of causal reasoning tasks across numerical simulations and real-world ecological video analysis (§ 4). We summarize the main contributions of this paper as follows:

- We reinterpret CRL using a *measurement model* framework, wherein the learned representations serve as proxy measurements for latent causal variables (§ 2). This formalism provides a clearer characterization of both the identification quality of learned representation and its usefulness for causal downstream tasks.
- We propose a new evaluation metric (T-MEX) that quantifies the alignment of the representations and the underlying measurement model (§ 3), and we demonstrate its advantages over widely used CRL evaluation metrics that suffer from notable limitations (App. D).
- Supported by theoretical analysis, our empirical evaluations confirm that T-MEX maintains validity and effectiveness across diverse causal reasoning scenarios, including treatment effect estimation and covariate adjustment in both numerical simulations and real-world ecological experiments (§ 4).

2. CRL from A Measurement Perspective

Notation. Please see App. A for a list of notations.

2.1. The Measurement Model Framework

We formulate causal representation learning using a measurement model framework inspired by the formalism of (Silva et al., 2006).

Definition 2.1 (Measurement model)**.** Let $\mathbf{V} = (\mathbf{Z}, \widehat{\mathbf{Z}})$ be a collection of variables that can be partitioned into two sets: a set of latent *causal variables* $\mathbf{Z} = \{\mathbf{Z}_1, \cdots, \mathbf{Z}_N\}$ with $\mathbf{Z}_i$ taking values in $\mathbb{R}$ for all $i \in [N]$, and a set of observed *measurement variables* $\widehat{\mathbf{Z}} = \{\widehat{\mathbf{Z}}_{A_1}, \cdots, \widehat{\mathbf{Z}}_{A_M}\}$ where for all $j \in [M]$, $\widehat{\mathbf{Z}}_{A_j}$ takes values in $\mathbb{R}^{D_j}$ with $D_j \in \mathbb{N}_+$, and it holds that $\widehat{\mathbf{Z}} \cap \mathbf{Z} = \varnothing$.

A *measurement model* $\mathcal{M} = \langle \mathbf{Z}, \widehat{\mathbf{Z}}, \{h_j\}_{j=1}^M \rangle$ specifies that $\widehat{\mathbf{Z}}$ follows a deterministic structural causal model

$$\left\{ \widehat{\mathbf{Z}}_{A_j} \coloneqq h_j(\mathbf{Z}_{\text{pa}(\widehat{\mathbf{Z}}_{A_j})}) \right\}_{j=1}^{M},$$

where $\text{pa}(\widehat{\mathbf{Z}}_{A_j}) \subseteq [N]$ for all $j \in [M]$, and $\mathbf{Z}_{\text{pa}(\widehat{\mathbf{Z}}_{A_j})} \subseteq \mathbf{Z}$ are called the causal parents of $\widehat{\mathbf{Z}}_{A_j}$. The functions h_j for all $j \in [M]$ are called the *measurement functions*. If for some $j \in [M]$, $|\text{pa}(\widehat{\mathbf{Z}}_{A_j})| = 1$ and the function h_j is the identity map, then the causal variable $\text{pa}(\widehat{\mathbf{Z}}_{A_j})$ is said to be *measured directly*. ♣

Definition 2.2 (Causally valid measurement model)**.** The measurement model (Defn. 2.1) is *"causally valid"* with respect to a statistical estimand g that identifies a target causal estimand, if the measurement $\widehat{\mathbf{Z}}$ is a drop-in replacement in g for the true causal variables $\mathbf{Z}$, i.e., $g(\mathbf{Z}) = g(\widehat{\mathbf{Z}})$. ♣

Further explanations and discussions on (causally valid) measurement models are provided in App. C.

3. Evaluating Causal Representations using Measurement Models

This section explains how the measurement model formalism we introduced in § 2 serves as a natural tool to evaluate causal representations. A causal representation is defined as a set of measurement variables output from an encoder — a parameterized function that maps the observables $\mathbf{X}$ to the measurement variables $\widehat{\mathbf{Z}}$. Each CRL method specifies

a measurement model, either through its identifiability guarantees or the particular causal task it addresses. This measurement model defines which causal variables a representation should *exclusively measure*. Given paired samples of the true causal variables $\mathbf{Z}$ and their corresponding measurement variables $\widehat{\mathbf{Z}}$ from a trained CRL model, evaluation boils down to comparing the measurement model against the observed joint distribution $P_{\mathbf{Z},\widehat{\mathbf{Z}}}$. We introduce additional statistical tests-related notations in App. B.

Exclusivity of measurements. A measurement model describes the relationship between the causal and the measurement variables. Specifically, it tell us for each measurement variable, which causal variables it should *exclusively measure*. We formally define this concept below.

Definition 3.1 (Exclusivity of a measurement variable)**.** Let $\mathcal{M} = \langle \mathbf{Z}, \widehat{\mathbf{Z}}, \{h_j\}_{j\in[M]} \rangle$ be a measurement model, if a measurement variable $\widehat{\mathbf{Z}}_{A_j}, j \in [M]$ only has one causal parent $\mathbf{Z}_i$ for some $i \in [N]$, then we say $\widehat{\mathbf{Z}}_{A_j}$ *exclusively measures* $\mathbf{Z}_i$. ♣

Given samples of the causal and measurement variables $\{(\mathbf{z}^k, \hat{\mathbf{z}}^k)\}_{k\in[n]}$, we can check whether the measurement variables do satisfy the exclusivity property in the data by testing the following null hypotheses:

$$\mathcal{H}_0(i,j) : \widehat{\mathbf{Z}}_{A_j} \perp\!\!\!\perp \mathbf{Z}_i \,\big|\, \mathbf{Z}_{[N]\setminus\{i\}}, \tag{3.1}$$

for all $i \in [N]$ and $j \in [M]$. For a numerical summary of the overall exclusivity, we propose the following *Test-based Measurement EXclusivity (T-MEX)* score.

Definition 3.2 (Test-based measurement exclusivity score)**.** Let $V \in \{0,1\}^{N\times M}$ be the adjacency matrix corresponding to the conditional independencies according to a measurement model $\mathcal{M}$, such that for all $j \in [M]$ and $i \in [N]$, $V_{ji} = 1$ if a causal variable $\mathbf{Z}_i$ is a causal parent of a measurement variable $\widehat{\mathbf{Z}}_{A_j}$ according to the measurement model, and $V_{ji} = 0$ otherwise. Let $\widehat{W} \in \{0,1\}^{N\times M}$ be the matrix constructed according to the test results of the conditional independencies in Equation (3.1) based on the samples of $(\mathbf{Z}, \widehat{\mathbf{Z}})$, such that for all $j \in [M]$ and $i \in [N]$, $\widehat{W}_{ji} = 1$ if $\mathcal{H}_0(i,j)$ is rejected, and $\widehat{W}_{ji} = 0$ otherwise. Then the test-based measurement exclusivity (T-MEX) score is defined as the *hamming distance* between V and $\widehat{W}$:

$$\text{T-MEX}(V, \widehat{W}) := \sum_{j=1}^{M} \sum_{i=1}^{N} \mathbb{1}(V_{ji} \neq \widehat{W}_{ji}),$$

where $\mathbb{1}$ denotes the indicator function. ♣

Details for computing T-MEX is given in Alg. 1. As T-MEX score is based on conditional independence testing, its value depends on the randomness in the samples, and the properties of the statistical tests being used. In Prop. 3.1, we show the upper bound of the expected T-MEX score when the joint distribution $P_{\mathbf{Z},\widehat{\mathbf{Z}}}$ of the causal variables $\mathbf{Z}$ and output measurement variables $\widehat{\mathbf{Z}}$ from a CRL model does align with a measurement model.

Proposition 3.1. *Let $\{\varphi_{ij}\}_{i\in[N],j\in[M]}$ be a family of tests for Equation (3.1) where for all $i \in [N]$ and $j \in [M]$, φ_{ij} is valid with level $\alpha \in (0,1)$ and has power at least $\beta \in (0,1)$. Given an adjacency matrix $V \in \{0,1\}^{N\times M}$ based on a measurement model, if the joint distribution $P_{\mathbf{Z},\widehat{\mathbf{Z}}}$ of the causal and measurement variables does align with the measurement model, and each entry in $\widehat{W}$ is computed based on an independent set of samples $\{(\mathbf{z}^k, \hat{\mathbf{z}}^k)\}_{k\in[n_{ij}]}, n_{ij} \in \mathbb{N}_+$, then it holds that $\mathbb{E}[\text{T-MEX}(V, \widehat{W})] \leq \alpha \cdot (MN - ||V||_1) + (1-\beta) \cdot ||V||_1$, where $||V||_1 = \sum_{i=1}^{N}\sum_{j=1}^{M} V_{ij}$ is the L_1-norm of V.*

4. Experiments

This section demonstrates the validity of the proposed T-MEX score in various causal reasoning settings. We first focus on *covariate adjustment* in numerical simulations, using T-MEX to evaluate both identifiability (Defn. B.1) and causal validity (Defn. 2.2) of the representations (§ 4.1). Next, we move on to *treatment effect estimation* in high-dimensional ecological video analysis, where we demonstrate that T-MEX effectively characterizes how well the learned representation supports answering downstream causal questions (§ 4.2). For both experiments, we estimate T-MEX based on the projected covariance measure (PCM) test (Lundborg et al., 2024) implemented in `pycomets` (Huang and Kook, 2025), which is an algorithm-agnostic test for conditional independence (see App. G for more explanations). Further experiment details and additional results are deferred to App. F.

4.1. Numerical Simulation

Experiment settings. We generate five causal variables, $\mathbf{Z}_i$ for $i \in [5]$ according to a linear structural causal model (see App. F.1), where two of the causal variables, $\mathbf{Z}_4$ and $\mathbf{Z}_5$, are *observed* (also termed "*directly measured*" in Defn. 2.1). The entangled observations $\mathbf{X} := f(\mathbf{Z}_1, \mathbf{Z}_2, \mathbf{Z}_3)$ are generated by applying a diffeomorphism $f : \mathbb{R}^3 \to \mathbb{R}^3$, implemented as an invertible MLP, on the causal variables. Our *target causal task is to estimate the ATE of $\mathbf{Z}_4$ on $\mathbf{Z}_5$*. As the true causal relationship between $\mathbf{Z}_4$ and $\mathbf{Z}_5$ is linear, we can construct a consistent causal estimator where $\mathbf{Z}_1$ is adjusted using linear regression, which is invariant up to *bijective transformations* of $\mathbf{Z}_1$ (App. H). Although $\mathbf{Z}_1$ is latent and cannot be directly adjusted for, one can *measure* it through a bijective transformation $\widehat{\mathbf{Z}}_{A_1} := h(\mathbf{Z}_1)$ which is obtained from the entangled observation $\mathbf{X}$. Note that in this case, $\widehat{\mathbf{Z}}_{A_1}$ *exclusively measures* (Defn. 3.1) the confounder $\mathbf{Z}_1$, as depicted

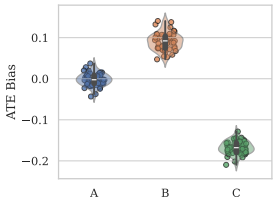

Figure 2: *T-MEX tracks the absolute bias of the ATE estimates* of $\mathbf{Z}_4$ on $\mathbf{Z}_5$ where $\widehat{\mathbf{Z}}_1$ is conditioned on as the back door adjustment.

in Fig. 4. We train three different CRL models based on the identifiable learning algorithm proposed by Yao et al. (2024b) and obtain samples of the measurement variable $\widehat{\mathbf{Z}}_{A_1}$. See Tab. 1 for details about model configurations.

Table 1: T-MEX and R^2 scores of the learned representations (presented as `mean±std`) of **model A** (sufficiently trained, i.e., $\widehat{\mathbf{Z}}_1$ exclusively measures $\mathbf{Z}_1$), **model B** (insufficiently trained model with unclear latent-measurement correspondence) and **model C** (manually corrupted representation by linearly mixing Z_2, Z_3 with the representation of model A) based on 50 simulated datasets, where each dataset contains 4096 observations.

Model	T-MEX (↓)	R^2		
		$\mathbf{Z}_1$	$\mathbf{Z}_2$	$\mathbf{Z}_3$
A	0.1200 ± 0.3283	0.9984 ± 0.0001	0.7516 ± 0.0064	0.8001 ± 0.0006
B	1.1800 ± 0.3881	0.6665 ± 0.0078	0.8305 ± 0.0032	0.8707 ± 0.0027
C	2.0000 ± 0.0000	0.9394 ± 0.0016	0.5421 ± 0.0096	0.6627 ± 0.0084

Results. Tab. 1 summarizes the T-MEX scores together with the coefficient of determination R^2 for all three models A, B and C, presented as `mean±sd`. *For statistical validity*, we compute the results using 50 simulated datasets from each model, with each dataset containing 4096 observations. Further details about the test results are provided in App. F.1. Tab. 1 shows that a sufficiently trained model (Model A) achieves a low T-MEX score, indicating that the learned representation $\widehat{\mathbf{Z}}_{A_1}$ exclusively measures the latent variable $\mathbf{Z}_1$. In contrast, the insufficiently trained and corrupted models (Models B and C) exhibit high T-MEX scores, demonstrating misalignment between the learned representation and the hypothesized measurement model (Fig. 4). Fig. 2 presents the ATE bias estimated from the learned representations of all three models. We observe a strong correlation between T-MEX and the absolute bias of the ATE, validating T-MEX as a reliable indicator of the causal validity of the learned representation (Defn. 2.2), whereas R^2 fails to show a clear correspondence with the ATE bias because R^2 was relatively high for all three latent variables as shown in Tab. 1.

4.2. Real-world Ecological Experiment: ISTAnt

Experiment settings. This experiment validates the T-MEX score on ISTAnt (Cadei et al., 2024), a real-world

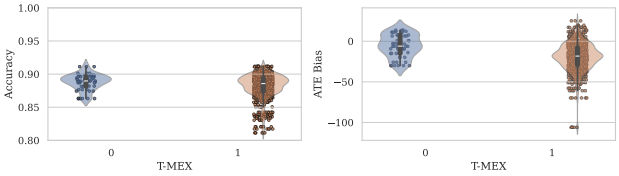

Figure 3: *T-MEX reflects model performance in terms of both classification accuracy and causal validity (Defn. 2.2).* Compared to their counterparts, models with lower T-MEX achieve consistently high accuracy (*Left*) and center their ATE bias near zero with reduced variance (*Right*).

ecological benchmark designed for treatment effect estimation. ISTAnt consists of video recordings of ant triplets with occasional grooming behavior. *The goal is to extract a per-frame representation for supervised behavior classification (grooming or not) to estimate the ATE of an intervention (exposure to a certain pathogen).* Retrieving causally valid representations in this case is challenging as we have more non-annotated than annotated data, as described by (Cadei et al., 2024). Fig. 5 depicts the hypothesized measurement model for this particular causal task, note that the treatment $\mathbf{T}$ and outcome $\mathbf{Y}$ are unconfounded because the data is collected through a randomized controlled trial, meaning that the binary treatment $\mathbf{T}$ is randomly assigned.

Results. We compute the T-MEX score for 2,400 different models at a significance level of $\alpha = 0.05$, and compare both classification accuracy and ATE bias against T-MEX. A full description of the considered models and training details is reported in App. F.2. We only focus on the models that yield an accuracy over 80% for meaningful statements. We observe that models with T-MEX = 0 achieve higher mean and lower variance for both accuracy and ATE bias, demonstrating that T-MEX effectively and reliably evaluates the quality of learned representations in terms of both classification performance and causal validity (Defn. 2.2).

5. Conclusion and Limitations

This paper reinterprets CRL from a measurement model perspective, where causal representations are treated as proxy measurements of latent causal variables (§ 2). This perspective provides a flexible framework that unites CRL identification theory with downstream task assumptions via measurement functions, yielding a principled way to evaluate representation quality – the Test-based Measurement EXclusivity (T-MEX) score (§ 3). We demonstrate in § 4 that our proposed T-MEX score effectively quantifies the identification and causal validity of the learned representation (Defn. 2.2). This provides a convenient and practical evaluation scheme for representation quality in real-world scenarios, especially when the true treatment effect bias is unavailable, such as in the absence of randomized studies.

ACKNOWLEDGMENT

This research was funded in whole or in part by the Austrian Science Fund (FWF) 10.55776/COE12. For open access purposes, the author has applied a CC BY public copyright license to any accepted manuscript version arising from this submission.

References

K. Ahuja, E. Caballero, D. Zhang, J.-C. Gagnon-Audet, Y. Bengio, I. Mitliagkas, and I. Rish. Invariance principle meets information bottleneck for out-of-distribution generalization. *Advances in Neural Information Processing Systems*, 34:3438–3450, 2021.

K. Ahuja, J. S. Hartford, and Y. Bengio. Weakly supervised representation learning with sparse perturbations. *Advances in Neural Information Processing Systems*, 35: 15516–15528, 2022.

K. Ahuja, A. Mansouri, and Y. Wang. Multi-domain causal representation learning via weak distributional invariances. In *International Conference on Artificial Intelligence and Statistics*, pages 865–873. PMLR, 2024.

C. Ai, L.-H. Sun, Z. Zhang, and L. Zhu. Testing unconditional and conditional independence via mutual information. *Journal of Econometrics*, 240(2):105335, 2024.

M. Arjovsky, L. Bottou, I. Gulrajani, and D. Lopez-Paz. Invariant risk minimization, 2020.

E. Bareinboim and J. Pearl. Causal inference and the data-fusion problem. *Proceedings of the National Academy of Sciences*, 113(27):7345–7352, 2016.

P. Billingsley. *Probability and Measure*. Wiley Series in Probability and Statistics. John Wiley & Sons, Hoboken, NJ, 4th edition, 2008.

S. Buchholz, G. Rajendran, E. Rosenfeld, B. Aragam, B. Schölkopf, and P. Ravikumar. Learning linear causal representations from interventions under general nonlinear mixing. *Advances in Neural Information Processing Systems*, 36, 2024.

R. Cadei, L. Lindorfer, S. Cremer, C. Schmid, and F. Locatello. Smoke and mirrors in causal downstream tasks. *Advances in Neural Information Processing Systems*, 37, 2024.

R. Cadei, I. Demirel, P. De Bartolomeis, L. Lindorfer, S. Cremer, C. Schmid, and F. Locatello. Causal lifting of neural representations: Zero-shot generalization for causal inferences. *arXiv preprint arXiv:2502.06343*, 2025.

A. C. Cameron and F. A. Windmeijer. An R-squared measure of goodness of fit for some common nonlinear regression models. *Journal of econometrics*, 77(2):329–342, 1997.

G. Casella and R. Berger. *Statistical inference*. CRC Press, 2024.

R. T. Chen, X. Li, R. B. Grosse, and D. K. Duvenaud. Isolating sources of disentanglement in variational autoencoders. *Advances in neural information processing systems*, 31, 2018.

V. Chernozhukov, D. Chetverikov, M. Demirer, E. Duflo, C. Hansen, W. Newey, and J. Robins. Double/debiased machine learning for treatment and structural parameters. *The Econometrics Journal*, 21(1):C1–C68, 2018.

X. Dong, B. Huang, I. Ng, X. Song, Y. Zheng, S. Jin, R. Legaspi, P. Spirtes, and K. Zhang. A versatile causal discovery framework to allow causally-related hidden variables. In *The Twelfth International Conference on Learning Representations*, 2024.

N. R. Draper and H. Smith. *Applied regression analysis*, volume 326. John Wiley & Sons, 1998.

C. Eastwood and C. K. Williams. A framework for the quantitative evaluation of disentangled representations. In *6th International Conference on Learning Representations*, 2018.

P. M. Faller, L. C. Vankadara, A. A. Mastakouri, F. Locatello, and D. Janzing. Self-compatibility: Evaluating causal discovery without ground truth. In *International Conference on Artificial Intelligence and Statistics*, pages 4132–4140. PMLR, 2024.

T. Fernández and N. Rivera. A general framework for the analysis of kernel-based tests. *Journal of Machine Learning Research*, 25(95):1–40, 2024.

M. Fumero, F. Wenzel, L. Zancato, A. Achille, E. Rodolà, S. Soatto, B. Schölkopf, and F. Locatello. Leveraging sparse and shared feature activations for disentangled representation learning. *Advances in Neural Information Processing Systems*, 36, 2024.

J. L. Gamella, S. Bing, and J. Runge. Sanity checking causal representation learning on a simple real-world system. *arXiv preprint arXiv:2502.20099*, 2025.

I. Higgins, L. Matthey, A. Pal, C. Burgess, X. Glorot, M. Botvinick, S. Mohamed, and A. Lerchner. beta-VAE: Learning basic visual concepts with a constrained variational framework. In *International conference on learning representations*, 2017.

S. Holm. A simple sequentially rejective multiple test procedure. *Scandinavian journal of statistics*, pages 65–70, 1979.

S. Huang and L. Kook. pycomets. https://github.com/shimenghuang/pycomets, 2025. Accessed: 2025-05-15.

A. Hyvärinen and P. Pajunen. Nonlinear independent component analysis: Existence and uniqueness results. *Neural networks*, 12(3):429–439, 1999.

A. Hyvarinen, H. Sasaki, and R. Turner. Nonlinear ICA using auxiliary variables and generalized contrastive learning. In *The 22nd International Conference on Artificial Intelligence and Statistics*, pages 859–868. PMLR, 2019.

M. Jain, A. Denton, S. Whitfield, A. Didolkar, B. Earnshaw, J. Hartford, et al. Automated discovery of pairwise interactions from unstructured data. *arXiv preprint arXiv:2409.07594*, 2024.

D. Janzing, D. Balduzzi, M. Grosse-Wentrup, and B. Schölkopf. Quantifying causal influences. *The Annals of Statistics*, 41(5):2324–2358, 2013.

H. Kim and A. Mnih. Disentangling by factorising. In *International conference on machine learning*, pages 2649–2658. PMLR, 2018.

L. Kong, S. Xie, W. Yao, Y. Zheng, G. Chen, P. Stojanov, V. Akinwande, and K. Zhang. Partial disentanglement for domain adaptation. In *International Conference on Machine Learning*, pages 11455–11472. PMLR, 2022.

L. Kong, B. Huang, F. Xie, E. Xing, Y. Chi, and K. Zhang. Identification of nonlinear latent hierarchical models. *arXiv preprint arXiv:2306.07916*, 2023.

L. Kook. Falsifying causal models via nonparametric conditional independence testing. In *Proceedings of the 39th International Workshop on Statistical Modelling (IWSM)*, 2025. (to appear).

L. Kook and A. R. Lundborg. Algorithm-agnostic significance testing in supervised learning with multimodal data. *Briefings in Bioinformatics*, 25(6):bbae475, 2024.

D. Krueger, E. Caballero, J.-H. Jacobsen, A. Zhang, J. Binas, D. Zhang, R. Le Priol, and A. Courville. Out-of-distribution generalization via risk extrapolation (rex). In *International conference on machine learning*, pages 5815–5826. PMLR, 2021.

A. Kumar, P. Sattigeri, and A. Balakrishnan. Variational inference of disentangled latent concepts from unlabeled observations. *arXiv preprint arXiv:1711.00848*, 2017.

S. Lachapelle, R. Pau, Y. Sharma, K. E. Everett, R. Le Priol, A. Lacoste, and S. Lacoste-Julien. Disentanglement via mechanism sparsity regularization: A new principle for nonlinear ICA. In *First Conference on Causal Learning and Reasoning*, 2022.

S. Lachapelle, T. Deleu, D. Mahajan, I. Mitliagkas, Y. Bengio, S. Lacoste-Julien, and Q. Bertrand. Synergies between disentanglement and sparsity: Generalization and identifiability in multi-task learning. In *International Conference on Machine Learning*, pages 18171–18206. PMLR, 2023.

P. Lippe, S. Magliacane, S. Löwe, Y. M. Asano, T. Cohen, and E. Gavves. Causal representation learning for instantaneous and temporal effects in interactive systems. In *The Eleventh International Conference on Learning Representations*, 2022a.

P. Lippe, S. Magliacane, S. Löwe, Y. M. Asano, T. Cohen, and S. Gavves. Citris: Causal identifiability from temporal intervened sequences. In *International Conference on Machine Learning*, pages 13557–13603. PMLR, 2022b.

F. Locatello, S. Bauer, M. Lucic, G. Raetsch, S. Gelly, B. Schölkopf, and O. Bachem. Challenging common assumptions in the unsupervised learning of disentangled representations. In *International Conference on Machine Learning*, pages 4114–4124. PMLR, 2019.

F. Locatello, S. Bauer, M. Lucic, G. Rätsch, S. Gelly, B. Schölkopf, and O. Bachem. A sober look at the unsupervised learning of disentangled representations and their evaluation. *Journal of Machine Learning Research*, 21(209):1–62, 2020.

A. R. Lundborg, I. Kim, R. D. Shah, and R. J. Samworth. The projected covariance measure for assumption-lean variable significance testing. *The Annals of Statistics*, 52 (6):2851–2878, 2024.

H. B. Mann and D. R. Whitney. On a test of whether one of two random variables is stochastically larger than the other. *The Annals of Mathematical Statistics*, pages 50–60, 1947.

M. Oquab, T. Darcet, T. Moutakanni, H. Vo, M. Szafraniec, V. Khalidov, P. Fernandez, D. Haziza, F. Massa, A. El-Nouby, et al. Dinov2: Learning robust visual features without supervision. *arXiv preprint arXiv:2304.07193*, 2023.

J. Pearl and D. Mackenzie. *The book of why: the new science of cause and effect*. Basic books, 2018.

J. Peters, J. M. Mooij, D. Janzing, and B. Schölkopf. Causal discovery with continuous additive noise models. *Journal of Machine Learning Research*, 2014.

J. Peters, D. Janzing, and B. Schlkopf. *Elements of Causal Inference: Foundations and Learning Algorithms*. The MIT Press, 2017. ISBN 0262037319.

A. Ravuri, K. Ulicna, J. Osea, K. Donhauser, and J. Hartford. Weakly supervised latent variable inference of proximity bias in crispr gene knockouts from single-cell images. In *Learning Meaningful Representations of Life (LMRL) Workshop at ICLR 2025*, 2025.

K. Ridgeway and M. C. Mozer. Learning deep disentangled embeddings with the F-statistic loss. *Advances in neural information processing systems*, 31, 2018.

J. M. Robins, A. Rotnitzky, and L. P. Zhao. Estimation of regression coefficients when some regressors are not always observed. *Journal of the American statistical Association*, 89(427):846–866, 1994.

M. Rojas-Carulla, B. Schölkopf, R. Turner, and J. Peters. Invariant models for causal transfer learning. *Journal of Machine Learning Research*, 19(36):1–34, 2018.

J. Runge. Conditional independence testing based on a nearest-neighbor estimator of conditional mutual information. In A. Storkey and F. Perez-Cruz, editors, *Proceedings of the Twenty-First International Conference on Artificial Intelligence and Statistics*, volume 84 of *Proceedings of Machine Learning Research*, pages 938–947. PMLR, 09–11 Apr 2018.

B. Schölkopf, F. Locatello, S. Bauer, N. R. Ke, N. Kalchbrenner, A. Goyal, and Y. Bengio. Toward causal representation learning. *Proceedings of the IEEE*, 109(5): 612–634, 2021.

R. D. Shah and J. Peters. The hardness of conditional independence testing and the generalised covariance measure. *The Annals of Statistics*, 48(3):1514–1538, 2020.

S. Shimizu, P. O. Hoyer, A. Hyvärinen, A. Kerminen, and M. Jordan. A linear non-gaussian acyclic model for causal discovery. *Journal of Machine Learning Research*, 7(10), 2006.

R. Silva, R. Scheines, C. Glymour, P. Spirtes, and D. M. Chickering. Learning the structure of linear latent variable models. *Journal of Machine Learning Research*, 7 (2), 2006.

C. Squires, A. Seigal, S. S. Bhate, and C. Uhler. Linear causal disentanglement via interventions. In *International Conference on Machine Learning*, volume 202, pages 32540–32560. PMLR, 2023.

E. V. Strobl, K. Zhang, and S. Visweswaran. Approximate kernel-based conditional independence tests for fast non-parametric causal discovery. *Journal of Causal Inference*, 7(1):20180017, 2019.

Y. Sun, L. Kong, G. Chen, L. Li, G. Luo, Z. Li, Y. Zhang, Y. Zheng, M. Yang, P. Stojanov, et al. Causal representation learning from multimodal biomedical observations. In *The Thirteenth International Conference on Learning Representations*, 2025.

B. Varici, E. Acartürk, K. Shanmugam, and A. Tajer. General identifiability and achievability for causal representation learning. In *International Conference on Artificial Intelligence and Statistics*, pages 2314–2322. PMLR, 2024.

J. von Kügelgen, Y. Sharma, L. Gresele, W. Brendel, B. Schölkopf, M. Besserve, and F. Locatello. Self-supervised learning with data augmentations provably isolates content from style. *Advances in Neural Information Processing Systems*, 34:16451–16467, 2021.

J. von Kügelgen, M. Besserve, L. Wendong, L. Gresele, A. Kekić, E. Bareinboim, D. Blei, and B. Schölkopf. Nonparametric identifiability of causal representations from unknown interventions. *Advances in Neural Information Processing Systems*, 36, 2024.

F. Xie, B. Huang, Z. Chen, R. Cai, C. Glymour, Z. Geng, and K. Zhang. Generalized independent noise condition for estimating causal structure with latent variables. *Journal of Machine Learning Research*, 25(191):1–61, 2024.

D. Yao, C. Muller, and F. Locatello. Marrying causal representation learning with dynamical systems for science. *Advances in Neural Information Processing Systems*, 37, 2024a.

D. Yao, D. Xu, S. Lachapelle, S. Magliacane, P. Taslakian, G. Martius, J. von Kügelgen, and F. Locatello. Multi-view causal representation learning with partial observability. In *The Twelfth International Conference on Learning Representations*, 2024b.

D. Yao, D. Rancati, R. Cadei, M. Fumero, and F. Locatello. Unifying causal representation learning with the invariance principle. *The Thirteenth International Conference on Learning Representations*, 2025.

W. Yao, G. Chen, and K. Zhang. Temporally disentangled representation learning. *Advances in Neural Information Processing Systems*, 35:26492–26503, 2022.

J. Zhang, K. Greenewald, C. Squires, A. Srivastava, K. Shanmugam, and C. Uhler. Identifiability guarantees for causal disentanglement from soft interventions. *Advances in Neural Information Processing Systems*, 36, 2024a.

K. Zhang, J. Peters, D. Janzing, and B. Schölkopf. Kernel-based conditional independence test and application in causal discovery. *arXiv preprint arXiv:1202.3775*, 2012.

K. Zhang, M. Gong, P. Stojanov, B. Huang, Q. Liu, and C. Glymour. Domain adaptation as a problem of inference on graphical models. *Advances in Neural Information Processing Systems*, 33, 2020.

K. Zhang, S. Xie, I. Ng, and Y. Zheng. Causal representation learning from multiple distributions: A general setting. *Internatinal Conference on Machine Learning*, 2024b.

Y. Zheng, I. Ng, and K. Zhang. On the identifiability of nonlinear ICA: Sparsity and beyond. *Advances in neural information processing systems*, 35:16411–16422, 2022.

Y. Zheng, B. Huang, W. Chen, J. Ramsey, M. Gong, R. Cai, S. Shimizu, P. Spirtes, and K. Zhang. Causal-learn: Causal discovery in python. *Journal of Machine Learning Research*, 25(60):1–8, 2024.

Appendix

Table of Contents

A. Notation and Terminology

Throughout, we write $[N]$ as shorthand for the set $\{1, \dots, N\}$. Random vectors are denoted by bold uppercase letters (e.g. $\mathbf{Z}$) and their realizations by bold lowercase (e.g., $\mathbf{z}$), indexed by superscripts. For instance, n samples of $\mathbf{Z}$ are written as $\{\mathbf{z}^k\}_{k\in[N]}$. A vector $\mathbf{Z}$ can be sliced either by a single index $i \in [\dim(\mathbf{Z})]$ via $\mathbf{Z}_i$ or a index subset $A \subseteq [\dim(\mathbf{Z})]$ with $\mathbf{Z}_A := \{\mathbf{Z}_i : i \in A\}$. $P_{\mathbf{Z}}$ denotes the probability distribution of the random vector $\mathbf{Z}$ and $p_{\mathbf{Z}}(\mathbf{z})$ denotes the associated probability density function (We omit the subscription and write $p(\mathbf{z})$ when the context is clear). By default, a "measurable" function is *measurable* w.r.t. the Borel sigma algebras and is defined w.r.t. the Lebesgue measure.

We list the symbols as follows.

$\mathbf{Z}$	Causal variables
$\mathbf{X}$	Observables
D_j	Dimension of the representation $\widehat{\mathbf{Z}}_{A_j}$
N	Dimension of the causal variables $\mathbf{Z}$
n	Number of samples for the statistical tests for T-MEX
$\mathbb{P}(\cdot)$	Probability operator
$\mathbb{E}(\cdot)$	Expectation operator
$\mathbb{1}(\cdot)$	Indicator function

B. Preliminaries

Definition B.1 (Block-identifiability (von Kügelgen et al., 2021))**.** A set of latent variables $\mathbf{Z} \in \mathbb{R}^{d_z}$ is block-identified by a representation $\widehat{\mathbf{Z}} \in \mathbb{R}^{d_{\hat{z}}}$ if there exists a bijection $h : \mathbb{R}^{d_z} \to \mathbb{R}^{d_{\hat{z}}}$ such that $\widehat{\mathbf{Z}} = h(\mathbf{Z})$. ♣

Additional notation. Let $\mathbf{Z}_1$, $\mathbf{Z}_2$, and $\mathbf{Z}_3$ be three absolutely continuous random variables taking values in $\mathbb{R}^{d_{Z_1}}$, $\mathbb{R}^{d_{Z_2}}$, and $\mathbb{R}^{d_{Z_3}}$ respectively. We say that $\mathbf{Z}_1$ and $\mathbf{Z}_2$ are *conditionally independent* given $\mathbf{Z}_3$ if $p(\mathbf{Z}_1, \mathbf{Z}_2 \,|\, \mathbf{Z}_3) = p(\mathbf{Z}_1 \,|\, \mathbf{Z}_3)p(\mathbf{Z}_2 \,|\, \mathbf{Z}_3)$, and it is denoted as $\mathbf{Z}_1 \perp\!\!\!\perp \mathbf{Z}_2 \,|\, \mathbf{Z}_3$. A statistical test φ is a function that maps data to $\{0, 1\}$, e.g., $\varphi : \mathbb{R}^{n \times d_{Z_1}} \times \mathbb{R}^{n \times d_{Z_2}} \times \mathbb{R}^{n \times d_{Z_3}} \to \{0, 1\}$, where n denotes the number of samples. The test φ rejects a null hypothesis $\mathcal{H}_0$ if $\varphi(\mathbf{Z}_1, \mathbf{Z}_2, \mathbf{Z}_3) = 1$ and does not reject it if $\varphi(\mathbf{Z}_1, \mathbf{Z}_2, \mathbf{Z}_3) = 0$. Given a significance level $\alpha \in (0, 1)$, a test is said to be *valid* if it holds that $\sup_{P \in \mathcal{H}_0} \mathbb{P}(\varphi(\mathbf{Z}_1, \mathbf{Z}_2, \mathbf{Z}_3) = 1) \leq \alpha$, and it is said to have power $\beta \in (0, 1)$ against an alternative distribution $P \notin \mathcal{H}_0$ if $\mathbb{P}(\varphi(\mathbf{Z}_1, \mathbf{Z}_2, \mathbf{Z}_3) = 1) = \beta$.

C. Further Explanation and Remarks

C.1. Measurement Model (Defn. 2.1)

Remark C.1 (Difference from (Silva et al., 2006)). While we borrow the concept of a measurement model from Silva et al. (2006), our framework differs in two key aspects. First, Silva et al. (2006) aims to uncover relationships among latent causal variables by searching for pure measurements, i.e., a tree-structure in which latent nodes have fixed, noisy, low-dimensional observed children (measurements). In contrast, we interpret a given causal representation produced by a CRL algorithm as measurement variables and focus on evaluating their usefulness for specific causal tasks, which requires specification of a causal model. Second, Silva et al. (2006) assumes a linear latent structural causal model, whereas our framework imposes no parametric structural assumption on the latent causal variables. Rather, we specify the relationship between the causal variables and their measurements according to certain hypotheses, such as identification guarantees, prior knowledge, or assumptions for specific causal downstream tasks. As we will see in § 3, this also allows us to properly evaluate a learned CRL model. ♠

Remark C.2 (Noisy measurements). While we treat the measurement variables $\widehat{\mathbf{Z}}$ as noise-free nonlinear mixing of their causal parents, we can easily extend our framework to noisy measurements by considering the noise variables as additional latent causal variables. ♠

Example C.1. Assume by the identifiability theory of a specific CRL method that each $\widehat{\mathbf{Z}}_{A_j}$ block-identifies (see Defn. B.1 (von Kügelgen et al., 2021, Defn 4.1)) a subset of latent variables $\mathbf{Z}_{S_i}$ ($S_i \subseteq [N]$). Then for the measurement model $\mathcal{M} = \langle \mathbf{Z}, \widehat{\mathbf{Z}}, \{h_j\}_{j=1}^M \rangle$ it holds that: $\widehat{\mathbf{Z}}_{A_j} := h_j(\mathbf{Z}_{S_i})$, with $h_j : \mathbb{R}^{|S_i|} \to \mathbb{R}^{D_j}$ a diffeomorphism for all $j \in [M]$.

The measurement model induces a partial directed acyclic graph (DAG), that is, for any latent variable q that is block-identified (Defn. B.1) by A_j, there is an edge from the latent causal variable $\mathbf{Z}_q$ to the measurement variable $\widehat{\mathbf{Z}}_{A_j}$, and the measurement function h_j is a diffeomorphism. Illustrative examples are shown in Fig. 1 for different identifiability guarantees. ♦

Discussion. Note that a measurement model specified by certain identifiability theory (see Fig. 1) is a necessary but not sufficient condition for drop-in replacement of a variable with its identified counterpart in a causal inference engine (Pearl and Mackenzie, 2018) or a downstream causal estimand like *average treatment effect* (Robins et al., 1994). To this end, we introduce *causally valid measurement model*.

C.2. Causally Valid Measurement Model (Defn. 2.2)

Discussion. Causal validity of a measurement model with respect to a specific estimand boils down to the estimand being invariant with respect to the measurement function. As (von Kügelgen et al., 2024) already pointed out, identification of a latent causal variable up to a non-linear parameterization (i.e., block-identifiability (Defn. B.1)) does not allow average treatment effect estimation if either the treatment or outcome is a latent causal variable without additional information. For that, a direct measurement (see Defn. 2.1) as in (Cadei et al., 2024; 2025) is necessary; alternatively, one can choose an estimand that is invariant to non-linear invertible parameterizations, e.g., (conditional) mutual information (Janzing et al., 2013). As another example, a non-linear invertible parameterization is enough to model confounding variables (Yao et al., 2024a) and instruments, see H for extended discussions and examples. Finally, note that the causal validity of the measurement models does not always require one-to-one correspondence between the measurement variables and latent causal variables: When an estimand concerns a coarse-graining of a subset of variables, then a measurement model mixing the right subset of variables can still be causally valid. For example, the valid adjustment set $\mathbf{W}$ in Fig. 11 can contain two or more variables, which can remain entangled with each other in the learned representation $\widehat{\mathbf{W}} := h(\mathbf{W})$ as long as the measurement function h is invertible, see App. H for detailed derivations.

When is a measurement model "true"? Note that any causal model between learned representation can always be trivially formulated as a measurement model, with each identified representation variable corresponding to a latent causal variable (i.e., $\widehat{\mathbf{Z}}_1 \to \widehat{\mathbf{Z}}_2$ implicitly implies a measurement model $\widehat{\mathbf{Z}}_1 \leftarrow \mathbf{Z}_1 \to \mathbf{Z}_2 \to \widehat{\mathbf{Z}}_2$). Sometimes, by means of other assumptions, the latent causal model may not match one-to-one with the measurements; for example, see Fig. 1 (b). Our discussion on the measurement model only specifies the dependency between a learned representation and an (implicitly) assumed latent causal model. Following (Peters et al., 2014), we intend the latent causal model to be true if it agrees with the results of randomized studies in practice. If the latent causal model is true, then a causally valid measurement model is trivially also true.

D. Related Work: Flaws of Existing Evaluation Metrics for CRL

In this section, we cover the metrics that have been used by most papers proposing causal representation learning approaches (von Kügelgen et al., 2021; 2024; Zheng et al., 2022; Ahuja et al., 2024; 2022; Varici et al., 2024; Zhang et al., 2024a;b; Yao et al., 2024b; Lippe et al., 2022a;b; Lachapelle et al., 2022; 2023; Yao et al., 2022; Zhang et al., 2024a; Squires et al., 2023; Buchholz et al., 2024; Yao et al., 2025) to name a few. We highlight how these metrics are not immediately suitable to evaluate identification results in the presence of causal relations, making it difficult to compare models and requiring great care in the interpretation of the results that is often missed (Gamella et al., 2025).

Standard evaluation for latent variable identification in existing CRL works employs *coefficient of determination* R^2 (Defn. D.1), and *mean correlation coefficient* (Defn. D.2). However, when the latent variables are causally related, a high score of these two metrics does not indicate that the learned representations align with the measurement model we expect from the identifiability theory. Example D.1 illustrates this limitation of these two metrics under the presence of causal dependencies.

Example D.1. Assume that the latent causal variables $\mathbf{Z}$ in Fig. 1 (b) follow a linear Gaussian additive noise model. Specifically, the latent variables $\mathbf{Z}_1$ and $\mathbf{Z}_2$ are generated based on the following structural equation:

$$\mathbf{Z}_2 \coloneqq a \cdot \mathbf{Z}_1 + e \tag{D.1}$$

with $e \sim P_e$, $\mathbb{E}[e] = 0$ and $e \perp\!\!\!\perp \mathbf{Z}_1$. Suppose that the measurement model which induces Fig. 1 (b) specifies that the measurement function $h : \mathbb{R} \to \mathbb{R}$ is a diffeomorphism such that $\widehat{\mathbf{Z}}_{A_1} = h(\mathbf{Z}_1)$, that is, $\widehat{\mathbf{Z}}_{A_1}$ identifies $\mathbf{Z}_1$, while $\widehat{\mathbf{Z}}_{A_1}$ should not contain any additional information about $\mathbf{Z}_2$. ♦

Coefficient of determination. R^2 measures the proportion of the variation in the dependent variables explained by the regression model (Draper and Smith, 1998), formally defined as

Definition D.1 (Population R^2 score)**.** Let $(\mathbf{Z}_i, \widehat{\mathbf{Z}}_{A_j})$ be a pair of random variables both taking values in $\mathbb{R}$, $i \in [N], j \in [M]$. The coefficient of determination R^2 score for predicting $\mathbf{Z}_i$ from $\widehat{\mathbf{Z}}_{A_j}$ is defined as

$$R^2(\mathbf{Z}_i, \widehat{\mathbf{Z}}_{A_j}) \coloneqq \frac{\mathbb{V}(\mathbb{E}[\mathbf{Z}_i \mid \widehat{\mathbf{Z}}_{A_j}])}{\mathbb{V}(\mathbf{Z}_i)},$$

where $\mathbb{E}$ and $\mathbb{V}$ denote the expectation and variance operators, respectively. ♣

Problem of R^2 in Example D.1: Let $R^2(\mathbf{Z}_1, \widehat{\mathbf{Z}}_{A_1})$ denote the R^2 score as defined in Defn. D.1. Following the linear mechanism in Equation (D.1), $R^2(\mathbf{Z}_2, \widehat{\mathbf{Z}}_{A_1})$ can be expressed as

$$\begin{aligned} R^2(\mathbf{Z}_2, \widehat{\mathbf{Z}}_{A_1}) &= \frac{\mathbb{V}(\mathbb{E}[\mathbf{Z}_2 \mid \widehat{\mathbf{Z}}_{A_1}])}{\mathbb{V}(\mathbf{Z}_2)} = \frac{\mathbb{V}(\mathbb{E}[a\mathbf{Z}_1 + e \mid \widehat{\mathbf{Z}}_{A_1}])}{\mathbb{V}(a\mathbf{Z}_1 + e)} \\ &= \frac{a^2\mathbb{V}(\mathbb{E}[\mathbf{Z}_1 \mid \widehat{\mathbf{Z}}_{A_1}])}{a^2\mathbb{V}(\mathbf{Z}_1) + \mathbb{V}(e)} = \frac{a^2\mathbb{V}(\mathbf{Z}_1)}{a^2\mathbb{V}(\mathbf{Z}_1) + \mathbb{V}(e)} R^2(\mathbf{Z}_1, \widehat{\mathbf{Z}}_{A_1}). \end{aligned} \tag{D.2}$$

Depending on the noise level $\mathbb{V}(e)$, $R^2(\mathbf{Z}_2, \widehat{\mathbf{Z}}_{A_1})$ can be either close to $R^2(\mathbf{Z}_1, \widehat{\mathbf{Z}}_{A_1})$ when $\mathbb{V}(e) \ll a^2\mathbb{V}(\mathbf{Z}_1)$ or close to 0 when $\mathbb{V}(e)$ is significantly higher than $a^2\mathbb{V}(\mathbf{Z}_1)$; in either case it does not reflect whether $\widehat{\mathbf{Z}}_{A_1}$ identifies $\mathbf{Z}_2$ or not, in the sense of Defn. B.1. Ultimately, R^2 is a metric for predictability, not for identifiability. Using it as an identifiability metric under causal dependency can lead to misinterpretation (Gamella et al., 2025).

Remark D.1 (Other problems of R^2 score). R^2 is designed to measure how well a *linear* model fits between two random variables. When the fitted model is nonlinear, R^2 can yield values outside $[0, 1]$, which can be misleading. See also Cameron and Windmeijer (1997) for more details. ♠

Mean correlation coefficient (MCC). Intuitively, MCC measures the *component-wise correspondence* between the learned representation $\widehat{\mathbf{Z}}$ and the ground truth latent variables $\mathbf{Z}$. When using MCC, it is required to have the same latent and encoding dimensions. We restate the definition of the MCC as follows.

Definition D.2 (Mean correlation coefficient)**.**

$$\text{MCC} = \frac{1}{N} \max_{\pi \in \text{perm[N]}} \sum_{i=1}^{N} |\text{Corr}(\mathbf{Z}_i, \widehat{\mathbf{Z}}_{\pi(i)})|,$$

where $\text{Corr}(\cdot, \cdot)$ refers to the Pearson correlation under linear relationship and Spearman correlation in the nonlinear case. ♣

However, we notice that MCC cannot capture how well the representations are *disentangled*, misaligning with its original purpose of measuring *component-wise correspondence*. Assume in Fig. 1 (b) that $\widehat{\mathbf{Z}}_{A_1} = \widehat{\mathbf{Z}}_1$ and $\widehat{\mathbf{Z}}_{A_2} = [\widehat{\mathbf{Z}}_2, \widehat{\mathbf{Z}}_3]$. The learned representations $\widehat{\mathbf{Z}}_{A_j}$ are linear mappings of their causal parents $\mathbf{Z}_{\text{pa}(\widehat{\mathbf{Z}}_{A_j})}$:

$$\widehat{\mathbf{Z}}_1 = s \cdot \mathbf{Z}_1; \qquad \widehat{\mathbf{Z}}_2 = a \cdot \mathbf{Z}_2 + b \cdot \mathbf{Z}_3; \qquad \widehat{\mathbf{Z}}_3 = c \cdot \mathbf{Z}_2 + d \cdot \mathbf{Z}_3,$$

where $s, a, b, c, d \neq 0$. In this case, the MCC would obtain the highest value 1 although $\mathbf{Z}_2, \mathbf{Z}_3$ are still entangled in the learned representation $\hat{\mathbf{Z}}$, demonstrating that MCC is inadequate in evaluating element-wise identification under causal relations.

Evaluation of causal relations. Causal relations are usually evaluated with the standard metrics *Structural Hamming distance* (SHD). We remark that evaluating causal discovery on the learned representations should always be done in conjunction with latent variable identification, as it is possible to achieve a perfect SHD (i.e, zero) with entangled representations, using e.g., LiNGAM (Shimizu et al., 2006), as shown numerically in App. F.3.

Evaluation of disentangled representation. Evaluating disentangled representations (where the ground truth latent variables are assumed to be mutually independent) is comparatively easier. In the disentangled case, the main objective is to assess how well the learned representation aligns one-to-one with the ground truth latents. Commonly used evaluation metrics for disentangled representations include the BetaVAE Score (Higgins et al., 2017), FactorVAE Score (Kim and Mnih, 2018), Mutual Information Gap (MIG Chen et al. (2018)), DCI-disentanglement (Eastwood and Williams, 2018), Modularity (Ridgeway and Mozer, 2018) and SAP (Kumar et al., 2017). Broadly, evaluating learned representations can be viewed as a two-stage procedure, first estimating the relationship between latent variables and representations, and then aggregating this information into a single score (Locatello et al., 2020). In some way, our test can be seen as following the same strategy, although evaluating variable-level correspondence is less straightforward given underlying causal relationships, making it a fundamentally more challenging and under-studied problem.

E. Proofs and Algorithms

This section includes the proof for Prop. 3.1 and the algorithm to compute the T-MEX score.

Proposition 3.1. *Let $\{\varphi_{ij}\}_{i\in[N],j\in[M]}$ be a family of tests for Equation (3.1) where for all $i \in [N]$ and $j \in [M]$, φ_{ij} is valid with level $\alpha \in (0, 1)$ and has power at least $\beta \in (0, 1)$. Given an adjacency matrix $V \in \{0, 1\}^{N\times M}$ based on a measurement model, if the joint distribution $P_{\mathbf{Z},\widehat{\mathbf{Z}}}$ of the causal and measurement variables does align with the measurement model, and each entry in $\widehat{W}$ is computed based on an independent set of samples $\{(\mathbf{z}^k, \hat{\mathbf{z}}^k)\}_{k\in[n_{ij}]}, n_{ij} \in \mathbb{N}_+$, then it holds that*

$$\mathbb{E}[\textit{T-MEX}(V, \widehat{W})] \leq \alpha \cdot (MN - ||V||_1) + (1 - \beta) \cdot ||V||_1,$$

where $||V||_1 = \sum_{i=1}^{N} \sum_{j=1}^{M} V_{ij}$ is the L_1-norm of V.

Remark E.1 (Intuition). Proposition 3.1 tells us that if the measurement model does hold for the joint distribution of the causal variables and the output representations from a trained CRL model, we would expect to see a "low" T-MEX score given that we employ valid statistical tests that are also powerful enough to reject the null under alternatives. A "low"

Algorithm 1: Compute T-MEX score from one set of samples

Input: Paired samples of causal variables and measurement variables $\{\mathbf{z}, \widehat{\mathbf{z}}_{A_1}, \ldots, \widehat{\mathbf{z}}_{A_M}\}$ where $\mathbf{z} \in \mathbb{R}^{n \times N}$ and $\widehat{\mathbf{z}}_{A_j} \in \mathbb{R}^{n \times D_j}$ for $j \in [M]$, adjacency matrix of the measurement model $V \in \{0,1\}^{N \times M}$, a set of statistical tests for $\{\varphi_{ij}\}_{i \in [N], j \in [M]}$ for (3.1), where for all $i \in [N], j \in [M]$, $\varphi_{ij} : \mathbb{R}^{n \times 1} \times \mathbb{R}^{n \times D_j} \times \mathbb{R}^{n \times (N-1)} \to \{0,1\}$

Output: T-MEX score of the given sample

$\widehat{W} \leftarrow \mathbf{0}^{N \times M}$

for $i \in [N]$ **do**

  for $j \in [M]$ **do**

    $\widehat{W}_{ij} \leftarrow \varphi_{ij}(\mathbf{z}_i, \widehat{\mathbf{z}}_{A_j}, \mathbf{z}_{[N] \setminus \{i\}})$

  end

end

return $\sum_{i=1}^{N} \sum_{j=1}^{M} \mathbb{1}(V_{ij} \neq \widehat{W}_{ij})$

T-MEX score does not in general refer to a 0 score, as it depends on V, the chosen significance level α, and the power of the test β. For example, let $\alpha = 0.05$, we consider a valid statistical test that has the highest power, i.e., $\beta = 1$, additionally, assume the number of 0s in V is 2, then the expected value of the T-MEX score is no larger than $0.05 \times 2 = 0.1$. ♠

Remark E.2 (Multiple testing). Prop. 3.1 assumes that each null hypothesis in Equation (3.1) is tested using an independent set of samples. When there is only one set of samples available for a large number of tests, using the same sample set can lead to inflation of the false positive rate, and may inflate the T-MEX score. In this case, we recommend doing a multiple comparison adjustment when constructing $\widehat{W}$, for example, the Bonferroni-Holm correction (Holm, 1979), which controls the family-wise error rate while it does not make assumptions on the dependencies of the multiple p-values. ♠

Remark E.3 (Nonparametric measurement model). In this section, we focus on the exclusivity perspective of a measurement model via an approach similar to the idea of falsification of causal graphs (e.g., Kook, 2025; Faller et al., 2024). This is a non-parametric approach which is agnostic to the measurement functions. In certain cases, however, a measurement model may contain not only the conditional independence structure, but also other parametric assumptions through specifications of the measurement functions $\{h_j\}_{j \in [M]}$. Then, one may extend T-MEX to also take these constraints into account. ♠

Proof. Suppose the joint distribution of $(\mathbf{Z}, \widehat{\mathbf{Z}})$ aligns with the conditional independencies indicated by the adjacency matrix V, that is, for all $i \in [N]$ and $j \in [M]$, if $V_{ij} = 0$, it holds that $\widehat{\mathbf{Z}}_{A_j} \perp\!\!\!\perp \mathbf{Z}_i \,|\, \mathbf{Z}_{[N] \setminus \{i\}}$; if $V_{ij} = 1$, it holds that $\widehat{\mathbf{Z}}_{A_j} \not\perp\!\!\!\perp \mathbf{Z}_i \,|\, \mathbf{Z}_{[N] \setminus \{i\}}$.

Fix a significance level $\alpha \in (0,1)$. Suppose for all $i \in [N]$ and all $j \in [M]$, the statistical test φ_{ij} is valid at level α and has powder at least $\beta \in [0,1]$ against the alternative distribution where $\widehat{\mathbf{Z}}_{A_j} \not\perp\!\!\!\perp \mathbf{Z}_i \,|\, \mathbf{Z}_{[N] \setminus \{i\}}$.

Then given independent sets of samples $\{\mathbf{z}^k, \hat{\mathbf{z}}^k\}_{k \in [n_{ij}]}$ for $i \in [N]$ and $j \in [M]$, and $\widehat{W}_{ij} = \varphi_{ij}(\mathbf{z}_i, \hat{\mathbf{z}}_{A_j}, \mathbf{z}_{[N] \setminus \{i\}})$, it holds that

- if $V_{ij} = 0$, then $P(\widehat{W}_{ij} = 1) \leq \alpha$;
- if $V_{ij} = 1$, then $P(\widehat{W}_{ij} = 0) \leq 1 - \beta$.

Therefore, the expected value of T-MEX score is given by

$$\begin{aligned} \mathbb{E}[T\text{-}MEX(V, \widehat{W})] &= \alpha \cdot \sum_{i,j} \mathbb{1}(V_{ij} = 0) + (1 - \beta) \sum_{i,j} \cdot \mathbb{1}(V_{ij} = 1) \\ &\leq \alpha \cdot (MN - ||V||_1) + (1 - \beta) \cdot ||V||_1 \end{aligned}$$

where $||V||_1$ is the 1-norm of V. The second inequality is implied by the that each test φ_{ij} is valid with level α and has power $\geq \beta$. □

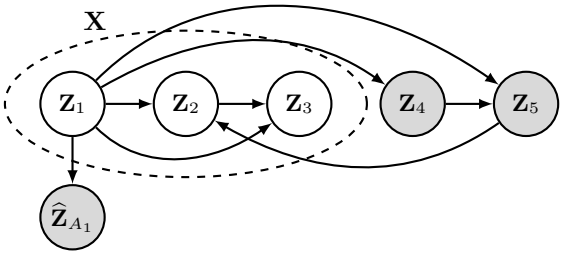

Figure 4: Measurement model containing the *latent* causal variables $\mathbf{Z}_1$, $\mathbf{Z}_2$, and $\mathbf{Z}_3$ (white nodes) and *observed* (also termed "*directly measured*" in Defn. 2.1) causal variables $\mathbf{Z}_4$ and $\mathbf{Z}_5$ (gray nodes). Entangled observable $\mathbf{X}$ is shown as a dashed oval. $\widehat{\mathbf{Z}}_{A_1}$ denotes the exclusive measurement (Defn. 3.1) of $\mathbf{Z}_1$.

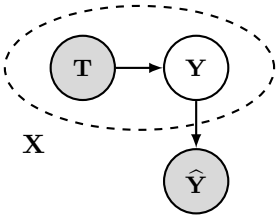

Figure 5: Measurement Model for the causal task in ISTAnt. $\mathbf{T}$ denotes the treatment (chemical exposure) and the *latent* outcome $\mathbf{Y}$ represents the ant's grooming behavior. Observable $\mathbf{X}$ (video recordings) is represented using a dashed oval. The measurement $\widehat{\mathbf{Y}}$ *exclusively measures* (Defn. 3.1) $\mathbf{Y}$.

F. Experiment Details and Additional Results

This section elaborates on the experiment settings of § 4. We include further information regarding the data-generating process for the simulated experiment (§ 4.1) and the ISTAnt dataset (Cadei et al., 2024) used in the ecological case study (§ 4.2), as well as additional experimental results.

F.1. Numerical Simulation

Experiment setting. We consider five causal variables $(\mathbf{Z}_1, \cdots, \mathbf{Z}_5)$ generated based on a linear structural causal model (Peters et al., 2017)

$$\mathbf{Z} = B\mathbf{Z} + \varepsilon,$$

where $\mathbf{Z} := (\mathbf{Z}_1, \mathbf{Z}_2, \mathbf{Z}_3, \mathbf{Z}_4, \mathbf{Z}_5)$, $\mathbf{Z}$ takes values in $\mathbb{R}^5$, $\varepsilon \sim \mathcal{N}_5(0, I)$, and $B = \begin{bmatrix} 0 & 0 & 0 & 0 & 0 \\ 1 & 0 & 0 & 0 & 1 \\ 1 & 1 & 0 & 0 & 0 \\ 1 & 0 & 0 & 0 & 0 \\ 1 & 0 & 0 & 1 & 0 \end{bmatrix}$, which induces the partial DAG depicted in Fig. 4. Two of the causal variables ($\mathbf{Z}_4$ and $\mathbf{Z}_5$) are observed (i.e., directly measured as in Defn. 2.1), and the other three ($\mathbf{Z}_1$, $\mathbf{Z}_2$, and $\mathbf{Z}_3$) are latent and we observe only a bijective mixing $\mathbf{X}$ of them.

For the purpose of latent variable identification, we consider the multiview scenario in (Yao et al., 2024b) where two views $\mathbf{X}_1, \mathbf{X}_2$ are generated from different subsets of latent variables. Formally, we have

$$\begin{aligned} \mathbf{X}_1 &= f_1(\mathbf{Z}_1, \mathbf{Z}_2) \\ \mathbf{X}_2 &= f_2(\mathbf{Z}_1, \mathbf{Z}_3), \end{aligned} \tag{F.1}$$

where $f_1, f_2 : \mathbb{R}^2 \to \mathbb{R}^2$ are diffeomorphisms, implemented using invertible MLPs as suggested by Yao et al. (2024b).

Implementation details. We employ the latent variable identification algorithm proposed by Yao et al. (2024b), which guarantees that the shared latent variables among different views can be identified up to a diffeomorphism in the sense of Defn. B.1. Thus, by utilizing $\mathbf{X}_1, \mathbf{X}_2$, we can obtain a nonlinear bijective transformation of their shared latent variable $\mathbf{Z}_1$. This allows us to construct a measurement model $\mathcal{M} = \langle \mathbf{Z}, \widehat{\mathbf{Z}}_{A_1}, \{h_1\} \rangle$ (see Fig. 4), where $\mathbf{Z} = \{\mathbf{Z}_1, \cdots, \mathbf{Z}_5\}$ and $\widehat{\mathbf{Z}}_{A_1} = h(\mathbf{Z}_1)$ for some (unknown) smooth invertible map $h : \mathbb{R} \to \mathbb{R}$.

We train three CRL models following the implementation settings in (Yao et al., 2024b, Tab. 4).

- **Model A**: a sufficiently trained model (trained for 50001 steps) from which we expect the learned representation $\widehat{\mathbf{Z}}^A_{A_1}$ (where by a slight abuse of notation, the superscript represents the model indicator) to *exclusively measure* $\mathbf{Z}_1$;
- **Model B**: an insufficiently trained model (trained for 51 steps) with unclear latent-measurement correspondence;

- **Model C**: a corrupted version of Model A where the representation $\widehat{\mathbf{Z}}^C_{A_1} := \widehat{\mathbf{Z}}^A_{A_1} + 0.2\mathbf{Z}_2 - 0.1\mathbf{Z}_3$, i.e., a linear mixing of the representation $\widehat{\mathbf{Z}}^A_{A_1}$ from Model A, and $\mathbf{Z}_2, \mathbf{Z}_3$.

For each of the three trained models, we generate 50 independent datasets, each containing 4096 paired samples of $\mathbf{Z}, \widehat{\mathbf{Z}}_{A_1}$. We compute the respective T-MEX scores based on these generated datasets for all three models, using the the projected covariance measure (PCM, Lundborg et al., 2024) implemented in `pycomets` (Huang and Kook, 2025) using linear regression models to estimate the conditional means (see App. G).

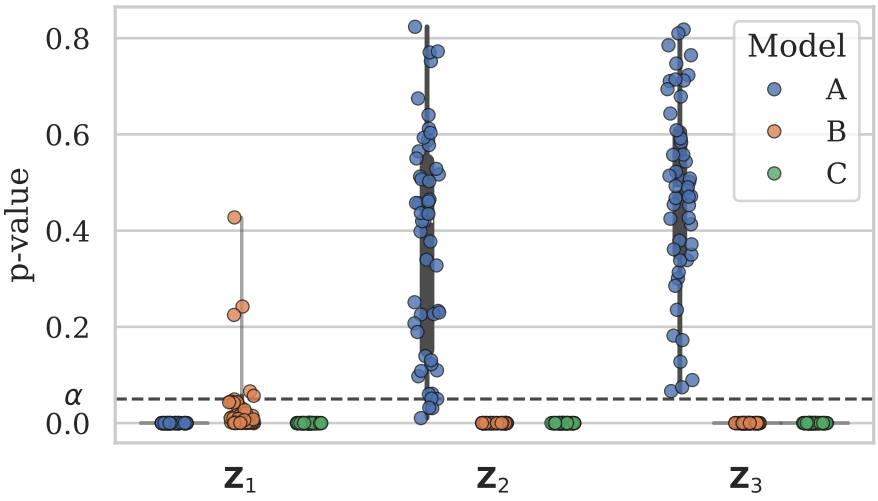

Figure 6: Violin plots of p-values from testing the conditional independencies $\widehat{\mathbf{Z}}_{A_1} \perp\!\!\!\perp \mathbf{Z}_i \,|\, \mathbf{Z}_{[5]\setminus i}$ for $i \in [3]$ based on the PCM tests (Lundborg et al., 2024). The black dashed line is at the significance level $\alpha = 0.05$. A p-value $< \alpha$ for $\mathbf{Z}_i$ means there is an edge from $\mathbf{Z}_i$ to the measurement $\widehat{\mathbf{Z}}_{A_1}$.

Additional results. Since T-MEX relies on statistical testing, we further assess its statistical validity by examining the underlying p-values that lead to the test results and the T-MEX score. Fig. 6 shows the p-values resulted from testing each of the three null hypotheses:

$$\mathcal{H}_0(i) : \widehat{\mathbf{Z}}_{A_1} \perp\!\!\!\perp \mathbf{Z}_i \,|\, \mathbf{Z}_{[5]\setminus i} \text{ for } i \in [3].$$

We omit $\mathbf{Z}_4$ and $\mathbf{Z}_5$ since they are not involved in generating the two views $\mathbf{X}_1$ and $\mathbf{X}_2$.

Fig. 6 shows that Model A aligns with the measurement model in Fig. 4, evidenced by (i) small p-values for $\mathcal{H}_0(1)$ and (ii) approximately uniformly distributed p-values for both $\mathcal{H}_0(2)$ and $\mathcal{H}_0(3)$, given a valid test (see App. G for further explanations). In contrast, for Models B and C, nearly all p-values are smaller than α, leading to rejections of the null hypotheses, which indicates that the learned representation $\widehat{\mathbf{Z}}_{A_1}$ is a mixture of all three causal variables $\mathbf{Z}_1, \mathbf{Z}_2, \mathbf{Z}_3$, and thus fails to exclusively measure $\mathbf{Z}_1$.

Computational resources. We train the CRL models (model A, B, C) using a single node GPU (`NVIDIA GeForce RTX1080Ti`) with 10GB of RAM, 4 CPU cores for less than one GPU hour. ATE estimation and T-MEX computation take less than one minute on a standard CPU.

F.2. Real-World Ecological Experiment: ISTAnt

Experiment Setting. ISTAnt is a real-world ecological benchmark designed to evaluate learned representations on downstream causal inference tasks from high-dimensional observational data. It comprises 44 ant-triplet video recordings collected through a randomized controlled trial. This benchmark adopts the problem formulation introduced by Cadei et al. (2024), aiming to estimate the causal effect of specific treatments (e.g., chemical exposure) on ants social behavior, particularly grooming events. The experimental design and recording setup are shown in Fig. 7; for further details, refer to (Cadei et al., 2024, App. C).

Table 2: Hyperparameters for the real-world ecological experiment (§ 4.2 and App. F.2), giving rise to 2,400 model configurations in total. All other settings follow (Cadei et al., 2024, App. C).

Hyperparameter	Value(s)
Input Preprocessing	`YES` / `NO`
Number of Hidden Layers	1, 2
Batch Size	64, 128, 256
Adam: learning rate	5e-2, 1e-2, 5e-3, 1e-3, 5e-4
Training objective	Empirical Risk, Invariant Risk (Arjovsky et al., 2020), vREx (Krueger et al., 2021), Deconfounded Risk (Cadei et al., 2025)
# Seeds	0,1, ..., 9

In ISTAnt, each observation (video recording) i is associated with a treatment assignment $\mathbf{T}_i$ and a set of experimental covariates $\mathbf{W}_i$ (including experiment day, time of the day, batch, position within the batch, and annotator). However, only a subset of videos is annotated with the outcome of interest $\mathbf{Y}_i$ (i.e., grooming events), which hinders reliable causal inference at a population level, such as treatment effect estimation. To address this challenge, Cadei et al. (2024) proposes to train a classifier on top of a pre-trained feature extractor (e.g., DINOv2 (Oquab et al., 2023)) using this limited set of annotated samples, to impute missing labels while still enabling valid causal inference at the population level; specifically, for estimating the Average Treatment Effect (ATE).

Implementation details. Following (Cadei et al., 2024), we train 2,400 classification heads on top of DINOv2 (Oquab et al., 2023), varying the architecture and training settings, and estimate the causal effect using all video samples together with the predicted labels $\widehat{\mathbf{Y}}$s by AIPW estimator (Robins et al., 1994). The hyperparameter configurations are summarized in Tab. 2, with all other implementation details following (Cadei et al., 2024, App. C).

By contrasting with the measurement model depicted in Fig. 5, we compute the T-MEX scores for all 2,400 models. Since we focus on models with more than 80% prediction accuracy (§ 4.2), the null hypothesis $\widehat{\mathbf{Y}} \perp\!\!\!\perp \mathbf{Y} \,\big|\, \mathbf{T}$ is rejected in all cases, consistently indicating $\mathbf{Y} \to \widehat{\mathbf{Y}}$. Thus, we only focus on the following null hypothesis:

$$\mathcal{H}_0 : \widehat{\mathbf{Y}} \perp\!\!\!\perp \mathbf{T} \,\big|\, \mathbf{Y},$$

where $\widehat{\mathbf{Y}}$ denotes the predicted label and $\mathbf{Y}$ the ground truth one. A misalignment with the measurement model in Fig. 5 leads to rejecting $\mathcal{H}_0$, resulting T-MEX=1, whereas as a causally valid representation $\widehat{\mathbf{Y}}$ that exclusively measures $\mathbf{Y}$ gives rise to T-MEX=0. We summarize all results in Fig. 3 and provide extended discussions in § 4.2.

Statistical validation. To further assess the statistical significance between the T-MEX = 0 and T-MEX = 1 groups, we conduct a Mann-Whitney U test (Mann and Whitney, 1947) with the null hypothesis $\mathcal{H}_0 : \mathbb{E}\Big[|\text{ATE Bias}| \;\Big|\; \text{T-MEX} = 1\Big] \leq \mathbb{E}\Big[|\text{ATE Bias}| \;\Big|\; \text{T-MEX} = 0\Big]$. The resulting p-value of 0.0047 leads us to rejecting $\mathcal{H}_0$, providing strong evidence that the average absolute bias of the ATE for models with T-MEX = 1 is significantly higher than for those with T-MEX = 0. Overall, T-MEX shows a strong correlation with absolute bias of the ATE, validating its reliability as an evaluation metric for the causal validity of learned representations (Defn. 2.2).

Real-world implications of T-MEX. We emphasize that the proposed T-MEX score can be computed using only observational data, possibly with selection bias, as long as this selection bias does not change the conditional independence between measurements and causal variables. Instead, calculating the ATE bias as in (Cadei et al., 2024) requires a validation set that closely approximates the underlying population of the randomized controlled trial, a significantly stronger assumption that is often difficult to satisfy in real-world settings. Overall, T-MEX offers a convenient and accessible evaluation metric that reliably quantifies the usefulness of the learned representation for a causal downstream task, without the need for additional identifying assumptions.

Computational resources. We run all the analyses in § 4.2 using 48GB of RAM, 20 CPU cores, and a single node GPU (`NVIDIA GeForce RTX2080Ti`) for 24 GPU hours. Data preprocessing and feature extraction using DINOv2 account for the majority of the computational time, whereas classifier training, AIPW estimation, and the T-MEX test contribute negligibly by comparison.

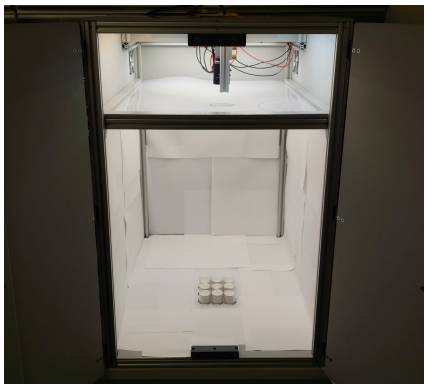

(a) Filming box

(b) Batch example

Figure 7: Visualization of ISTAnt recording set-up (Cadei et al., 2024).

F.3. Caveats of Using SHD to Evaluate Causal Representations

Experiment Setting. This experiment explores the potential pitfalls when directly using SHD to evaluate causal representations without properly evaluating the element-wise latent variable identification. Specifically, we consider a set of causal variables generated through the following structural equations:

$$\begin{aligned} \mathbf{Z}_1 &= \epsilon_1 \\ \mathbf{Z}_2 &= \alpha_{12} \cdot \mathbf{Z}_1 + \beta_2 \cdot \epsilon_2 \\ \mathbf{Z}_3 &= \alpha_{13} \cdot \mathbf{Z}_1 + \alpha_{23} \cdot \mathbf{Z}_2 + \beta_3 \cdot \epsilon_3, \end{aligned} \tag{F.2}$$

Assume the learned representation corresponds to the ground truth causal variable as follows:

$$\begin{aligned} \widehat{\mathbf{Z}}_{A_1} &= \gamma_1 \cdot \mathbf{Z}_1 + \gamma_{21} \cdot \mathbf{Z}_2 \\ \widehat{\mathbf{Z}}_{A_2} &= \gamma_2 \cdot \mathbf{Z}_2 \\ \widehat{\mathbf{Z}}_{A_3} &= \gamma_3 \cdot \mathbf{Z}_3 \end{aligned} \tag{F.3}$$

where $\widehat{\mathbf{Z}}_{A_1}$ remains a mixing of $\mathbf{Z}_1$ and $\mathbf{Z}_2$. The corresponding measurement model is shown in Fig. 8.

Implementation details. We generate 100 different structure and measurement models following Equations (F.2) and (F.3), with all coefficients αs and γs sampled from Unif$[1, 10]$ and the βs sampled from Unif$[0.005, 0.02]$. We run LiNGAM (Shimizu et al., 2006) from causal-learn (Zheng et al., 2024) to discover the causal relationships between the measurements $\widehat{\mathbf{Z}}_{A_1}, \widehat{\mathbf{Z}}_{A_2}, \widehat{\mathbf{Z}}_{A_3}$.

Results. Fig. 9 shows the structural hamming distance of between the discovered graph on $\widehat{\mathbf{Z}}$ and the ground truth one. Despite being entangled between $\mathbf{Z}_1, \mathbf{Z}_2$, $\widehat{\mathbf{Z}}$ still yield the correct causal graph in most of the cases (77%), as shown by the first bar in the plot. Hence, causal relations between the measurement variables should always be evaluated in conjunction with the variable identification. Otherwise, it can lead to misinterpretations as showcased by Fig. 9.

Computational resources. Data generating and causal discovery for App. F.3 in total takes less than 10 minutes on a standard CPU.

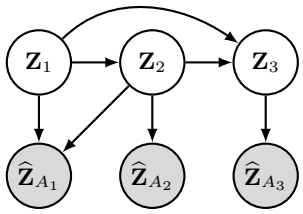

Figure 8: Example measurement model, where $\widehat{\mathbf{Z}}_{A_1}$ block-identifies $\mathbf{Z}_1, \mathbf{Z}_2$, $\widehat{\mathbf{Z}}_{A_2}$ and $\widehat{\mathbf{Z}}_{A_3}$ identifies $\mathbf{Z}_2, \mathbf{Z}_3$ respectively.

G. Background on Conditional Independence Testing

Testing conditional independence of two random variables $\mathbf{X}$ and $\mathbf{Y}$ given a third random variable $\mathbf{Z}$ is known to be a difficult problem if Z is a continuous variable (Shah and Peters, 2020). The goal of conditional independence test is to test the null hypothesis

$$\mathcal{H}_0 : \mathbf{X} \perp\!\!\!\perp \mathbf{Y} \,\big|\, \mathbf{Z}.$$

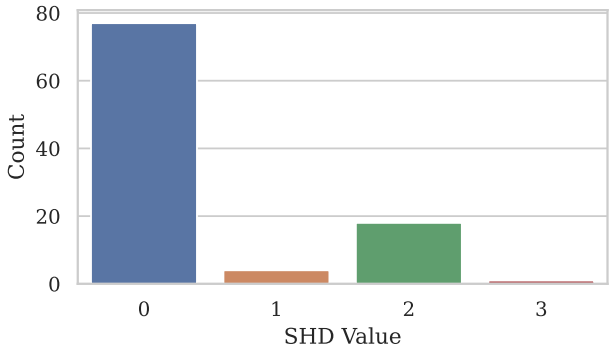

Figure 9: Structural Hamming Distance Values (SHD) of 100 structure and measurement models following Equations (F.2) and (F.3), where the measurement $\widehat{\mathbf{Z}}_{A_1}$ is a mixing of the ground truth latent $\mathbf{Z}_1, \mathbf{Z}_2$. SHDs are computed between the discovered graph on $\widehat{\mathbf{Z}}$ and the ground truth one.

Shah and Peters (2020) have shown that there is no valid test (i.e., a test that guarantees a Type I error rate to be no larger than the given significance level α) that has power against all alternatives.

Consider univariate variables $\mathbf{X}, \mathbf{Y}, \mathbf{Z}$, the generalized covariance measure (GCM) test proposed in Shah and Peters (2020) aims to test an implication of conditional independence which can be written as the following null hypothesis:

$$\mathcal{H}_0^{\text{GCM}} : \mathbb{E}[(\mathbf{Y} - \mathbb{E}[\mathbf{Y} \,|\, \mathbf{Z}])(\mathbf{X} - \mathbb{E}[\mathbf{X} \,|\, \mathbf{Z}])] = 0.$$

The validity of the GCM test thus relies on that the conditional means $\mathbb{E}[\mathbf{Y} \,|\, \mathbf{Z}]$ and $\mathbb{E}[\mathbf{X} \,|\, \mathbf{Z}]$ can be learned at sufficiently fast rates. It turns out that GCM does not have power against any alternative for which $\mathbb{E}[\text{Cov}(\mathbf{X}, \mathbf{Y} \,|\, \mathbf{Z})] = 0$ but $\mathbf{X} \not\perp\!\!\!\perp \mathbf{Y} \,|\, \mathbf{Z}$ (Lundborg et al., 2024).

The projected covariance measure (PCM) proposed by Lundborg et al. (2024) improves the power issue of GCM by testing a different implication of conditional independence:

$$\mathcal{H}_0^{\text{PCM}} : \mathbb{E}[\mathbf{Y} \,|\, \mathbf{X}, \mathbf{Z}] = \mathbb{E}[\mathbf{Y} \,|\, \mathbf{Z}].$$

Similar to GCM, to ensure its validity, PCM also requires that the conditional means can be learned sufficiently fast, which is satisfied in our experiments (§ 4).

There are other conditional independence tests such as mutual information based methods (Ai et al., 2024; Runge, 2018) and kernel-based methods (Fernández and Rivera, 2024; Strobl et al., 2019; Zhang et al., 2012). We opted for PCM in our experiments for its computational advantage and theoretical guarantees on its validity under a flexible, model-agnostic framework. More discussions on the usage of PCM and GCM can be found in Kook and Lundborg (2024). Notably, T-MEX is a general evaluation metric for causal representations that does not specify any particular type of tests, allowing practitioners to choose other testing methods that are more suitable for their problem settings.

H. Extended Discussion

This section elaborates on the implications of learned representations for downstream causal tasks. As briefly discussed in the main paper (following Defn. 2.2), a representation is *causally valid* (Defn. 2.2) with respect to a statistical estimand if and only if the statistical estimand remains unchanged when plugging in the measurement variables correspond to the causal variables. More concretely, we illustrate the implications of nonlinear invertible reparameterizations of causal variables in two commonly encountered scenarios: when representations serve as proxies of (i) the treatment or outcome variables, and (ii) the confounders or instrumental variables.

H.1. Representations of Treatment and Outcome

Assume in Fig. 10 that $\widehat{\mathbf{Z}}_{A_1}, \widehat{\mathbf{Z}}_{A_2}$ are element-wise nonlinear invertible reparametrization of $\mathbf{Z}_1, \mathbf{Z}_2$ respectively; i.e., $\forall i \in \{1,2\}, \widehat{\mathbf{Z}}_{A_i} = h_i(\mathbf{Z}_i)$ for some diffeomorphism $h_i : \mathbb{R} \to \mathbb{R}$. We aim to estimate the treatment effect of $\mathbf{Z}_1 \to \mathbf{Z}_2$ using the learned representations $\widehat{\mathbf{Z}}_{A_1}$ and $\widehat{\mathbf{Z}}_{A_2}$.

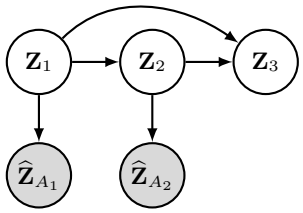

Figure 10: $\widehat{\mathbf{Z}}_{A_i}$ measures $\mathbf{Z}_i$ through a nonlinear bijection for both $i = 1, 2$.

Assume the $\mathbf{Z}_2$ is generated following Equation (D.1), i.e.,

$$\mathbf{Z}_2 \coloneqq a \cdot \mathbf{Z}_1 + e$$

with $e \sim P_e$, $\mathbb{E}[e] = 0$ and $e \perp\!\!\!\perp \mathbf{Z}_1$. Given there is no unobserved confounding, the ground truth average treatment effect is written as

$$\text{ATE}(\mathbf{Z}_1 \to \mathbf{Z}_2) = \frac{\partial \mathbb{E}[\mathbf{Z}_2 \mid do(\mathbf{Z}_1 = \mathbf{z}_1)]}{\partial \mathbf{z}_1} = \frac{\partial \mathbb{E}[\mathbf{Z}_2 \mid \mathbf{Z}_1 = \mathbf{z}_1]}{\partial \mathbf{z}_1} = \frac{\partial \mathbb{E}[a\mathbf{z}_1 + e]}{\partial \mathbf{z}_1} = a. \tag{H.1}$$

We assume measurement function h_i for all $i \in \{1,2\}$ to be linear, i.e.,

$$\widehat{\mathbf{Z}}_{A_1} = \alpha_1 \cdot \mathbf{Z}_1, \qquad \widehat{\mathbf{Z}}_{A_2} = \alpha_2 \cdot \mathbf{Z}_2, \quad \text{and} \quad \alpha_1, \alpha_2 \neq 0. \tag{H.2}$$

The ATE estimand from the learned representations yields:

$$\begin{aligned} \text{ATE}(\widehat{\mathbf{Z}}_{A_1} \to \widehat{\mathbf{Z}}_{A_2}) &= \frac{\partial \mathbb{E}[\widehat{\mathbf{Z}}_{A_2} \mid \widehat{\mathbf{Z}}_{A_1} = \hat{\mathbf{z}}_{A_1}]}{\partial \hat{\mathbf{z}}_{A_1}} \\ &= \frac{\partial \mathbb{E}[\alpha_2 \mathbf{Z}_2 \mid \alpha_1 \mathbf{Z}_1 = \alpha_1 \mathbf{z}_1]}{\partial \alpha_1 \mathbf{z}_1} \\ &= \frac{\alpha_2 \partial \mathbb{E}[\mathbf{Z}_2 \mid \mathbf{Z}_1 = \mathbf{z}_1]}{\alpha_1 \partial \mathbf{z}_1} = \frac{\alpha_2}{\alpha_1} a. \end{aligned} \tag{H.3}$$

As shown by Equation (H.3), the ATE estimand using the learned representation $\widehat{\mathbf{Z}}_{A_1}$ and $\widehat{\mathbf{Z}}_{A_2}$ can be arbitrarily scaled by the factor of α_2/α_1. Thus, measurements that bijectively transform the causal latent variables cannot naively support estimating the treatment effect, violating causal validity (Defn. 2.2); it requires direct supervision or observation on *both* treatment and outcome variables, as also pointed out by (von Kügelgen et al., 2024, Sec. 4).

On the other hand, information-theoretic measures for quantifying causal influence remain invariant under bijective transformation, such as the mutual information $I_{\text{int}}(\mathbf{Z}_1; \mathbf{Z}_2) = I_{\text{int}}(\widehat{\mathbf{Z}}_{A_1}; \widehat{\mathbf{Z}}_{A_2})$, as shown by Janzing et al. (2013).

H.2. Representations of Confounders or Instruments

Measuring confounding. We first show an example where an observed treatment $\mathbf{T}$ and an observed outcome $\mathbf{Y}$ is confounded by a third variable $\mathbf{W}$ which is measured by $\widehat{\mathbf{W}} = h(\mathbf{W})$ through a deterministic invertible function h.

Formally, the measurement model is defined as $\mathcal{M}^{\text{conf}} = \langle \mathbf{Z}, \widehat{\mathbf{Z}}, \{h\} \rangle$ with $\mathbf{Z} = \{\mathbf{T}, \mathbf{Y}, \mathbf{W}\}$ and $\widehat{\mathbf{Z}} = \{\widehat{\mathbf{W}}\}$, where $\mathbf{T}, \mathbf{Y}$ are *directly measured* (Defn. 2.1). The corresponding DAG is given in Fig. 11. We show in the following that this measurement model is indeed causally valid (Defn. 2.2) with respect to the statistical estimand for the Average Treatment Effect (ATE) of $\mathbf{T}$ on $\mathbf{Y}$.

Under the standard assumptions for backdoor adjustment, it follows that

$$\begin{aligned} \mathbb{E}(\mathbf{Y} | do(\mathbf{T} = t)) &= \mathbb{E}_{\mathbf{w}} \left[\mathbb{E}(\mathbf{Y} \mid \mathbf{W}, \mathbf{T} = t) \right] \\ &= \int \mathbb{E}(\mathbf{Y} \mid \mathbf{W}, \mathbf{T} = t) P(\mathbf{W}) d\mathbf{w} \\ &= \int \mathbb{E}(\mathbf{Y} \mid h^{-1}(\widehat{\mathbf{W}}), \mathbf{T} = t) P(h^{-1}(\widehat{\mathbf{W}})) \frac{dh^{-1}(\hat{\mathbf{w}})}{d\hat{\mathbf{w}}} d\hat{\mathbf{w}} \\ &= \int \mathbb{E}(\mathbf{Y} \mid \widehat{\mathbf{W}}, \mathbf{T} = t) P(\widehat{\mathbf{W}}) d\hat{\mathbf{w}} \\ &= \mathbb{E}_{\hat{\mathbf{w}}} \left[\mathbb{E}(\mathbf{Y} \mid \widehat{\mathbf{W}}, \mathbf{T} = t) \right], \end{aligned} \tag{H.4}$$

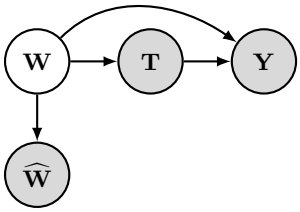

Figure 11: *ATE remains invariant under bijective transformation of confounders.* The treatment $\mathbf{T}$ and outcome $\mathbf{Y}$ are directly measured (i.e., observed) whereas confounder $\mathbf{W}$ is measured by $\widehat{\mathbf{W}}$ through a nonlinear bijection.

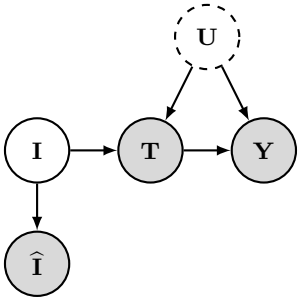

Figure 12: *ATE remains invariant under bijective transformation of instruments.* $\widehat{\mathbf{I}}$ measures the instrument variable $\mathbf{I}$ through a nonlinear bijection. The treatment $\mathbf{T}$ and outcome $\mathbf{Y}$ are directly measured (i.e., observed), and $\mathbf{U}$ denotes unobserved confounding.

where we used the change of variable formula and the fact that $\mathbb{E}(\mathbf{Y} \mid \widehat{\mathbf{W}}, \mathbf{T} = t) = \mathbb{E}(\mathbf{Y}|h^{-1}(\widehat{\mathbf{W}}), \mathbf{T} = t)$. This is because $h^{-1}(\widehat{\mathbf{W}})$ is a sufficient statistic for $\mathbf{W}$ (Casella and Berger, 2024, Ch. 6.2) following h is invertible.

Under the same assumptions, the ATE for *binary* treatment can then be identified by the following statistical estimand

$$\begin{aligned} \text{ATE}(\mathbf{T} \to \mathbf{Y}) &= \mathbb{E}[\mathbf{Y}|do(\mathbf{T} = 1)] - \mathbb{E}[\mathbf{Y} \mid do(\mathbf{T} = 0)] \\ &= \mathbb{E}_{\mathbf{w}} \left[\mathbb{E}(\mathbf{Y} \mid \mathbf{W}, \mathbf{T} = 1) - \mathbb{E}(\mathbf{Y} \mid \mathbf{W}, \mathbf{T} = 0)\right]. \end{aligned} \tag{H.5}$$

Following Equation (H.4), we have

$$\text{ATE}(\mathbf{T} \to \mathbf{Y}) = \mathbb{E}_{\hat{\mathbf{w}}} \left[\mathbb{E}(\mathbf{Y} \mid \widehat{\mathbf{W}}, \mathbf{T} = 1) - \mathbb{E}(\mathbf{Y} \mid \widehat{\mathbf{W}}, \mathbf{T} = 0)\right],$$

indicating that the identified statistical estimand $\text{ATE}(\mathbf{T} \to \mathbf{Y})$ remains invariant for the measurement $\widehat{\mathbf{W}}$. Similarly, ATE also remains invariant when the treatment is continuous:

$$\text{ATE}(\mathbf{T} \to \mathbf{Y}) = \frac{\partial \mathbb{E}[\mathbf{Y} \mid do(\mathbf{T} = t)]}{dt} = \frac{\partial \mathbb{E}_{\mathbf{w}} \mathbb{E}[\mathbf{Y} \mid \mathbf{W}, \mathbf{T} = t]}{dt} = \frac{\partial \mathbb{E}_{\hat{\mathbf{w}}} \mathbb{E}[\mathbf{Y} \mid \widehat{\mathbf{W}}, \mathbf{T} = t]}{dt}, \tag{H.6}$$

where the last equality holds because of Equation (H.4). Therefore, we have shown that invertible reparameterizations of the confounders can be a drop-in replacement of the true confounding variables in the statistical estimand for ATE, for both discrete and continuous treatments, and thus this measurement model $\mathcal{M}^{\text{conf}}$ is indeed causally valid for ATE.

Measuring instrumental variables. We now give a second example of ATE estimation under an instrumental variable setup. We assume that the instrument $\mathbf{I}$ is measured by $\widehat{\mathbf{I}} = h(\mathbf{I})$ through a bijective transformation h. We show that under certain assumptions, the statistical estimand does not change when using $\widehat{\mathbf{I}}$ as a drop-in replacement of the true instrument $\mathbf{I}$. We focus on the case where the instrument $\mathbf{I}$, the treatment $\mathbf{T}$, and the response $\mathbf{Y}$ are all univariate continuous variables; further discussion on multivariate and discrete valued variables is beyond the scope of this paper. Formally, the measurement model is defined as $\mathcal{M}^{\text{IV}} = \langle \mathbf{Z}, \widehat{\mathbf{Z}}, \{h\} \rangle$ with causal variables $\mathbf{Z} = \{\mathbf{I}, \mathbf{T}, \mathbf{Y}\}$ and measurement variables $\widehat{\mathbf{Z}} = \{\widehat{\mathbf{I}}\}$. The treatment $\mathbf{T}$ and outcome $\mathbf{Y}$ are *directly measured* (Defn. 2.1) and confounded by unknown hidden confounders $\mathbf{U}$. Fig. 12 shows the DAG of this measurement model.

We show in the following that the instrument $\mathbf{I}$ remains a valid instrumental variable under a bijective transformation, i.e., the measurement variable $\widehat{\mathbf{I}} = h(\mathbf{I})$ also satisfies the standard IV assumptions, which are listed as follows:

- Relevancy: $\mathbf{I} \not\perp\!\!\!\perp \mathbf{T} \,\big|\, \mathbf{U}$
- Unconfoundedness: $\mathbf{I} \perp\!\!\!\perp \mathbf{U}$
- Exclusion restriction criteria: $\mathbf{I} \perp\!\!\!\perp \mathbf{Y} \,\big|\, \mathbf{T}, \mathbf{U}$

Following standard probability theory (see e.g., Billingsley, 2008), if h is a bijective function, all three conditions still hold when replacing $\mathbf{I}$ by $h(\mathbf{I})$. This means that if the ATE is identified by a statistical estimand when using $\mathbf{I}$ as an instrument, it is also identified when using $\widehat{\mathbf{I}}$ as an instrument. In other words, the measurement model $\mathcal{M}^{\text{IV}}$ is causally valid with respect to an identified statistical estimand because $\widehat{\mathbf{I}}$ can serve as a drop-in replacement for $\mathbf{I}$ (Defn. 2.2).

As a specific example, consider the case where the causal mechanism of $\mathbf{Y}$ is partially linear (a commonly studied setup in the semi-parametric inference literature, see e.g., Chernozhukov et al. (2018)), i.e., $\mathbf{Y} = \mathbf{T}\beta + g(\mathbf{U}, \varepsilon)$, for some measurable function g where $\mathbb{E}[g(\mathbf{U}, \epsilon)] = 0$ and where $\varepsilon \sim P_\varepsilon$ is an independent noise variable, the ATE

$$\text{ATE}(\mathbf{T} \to \mathbf{Y}) = \frac{\partial \mathbb{E}[\mathbf{Y} \mid do(\mathbf{T} = \mathbf{t})]}{\partial \mathbf{t}} = \frac{\partial \mathbb{E}[\mathbf{t}\beta + g(\mathbf{U}, \varepsilon)]}{\partial \mathbf{t}} = \beta$$

can be identified by the statistical estimand

$$\text{ATE}(\mathbf{T} \to \mathbf{Y}) = \frac{\text{Cov}(\mathbf{Y}, \mathbf{I})}{\text{Cov}(\mathbf{T}, \mathbf{I})}. \tag{H.7}$$

We show in the following that the statistical estimand $\text{ATE}(\mathbf{T} \to \mathbf{Y})$ in Equation (H.7) remains invariant when using $\widehat{\mathbf{I}}$ as a drop-in replacement for $\mathbf{I}$. Plugging in $\widehat{\mathbf{I}}$ in the numerator

$$\text{Cov}(\mathbf{Y}, \widehat{\mathbf{I}}) = \mathbb{E}[\mathbf{Y}\widehat{\mathbf{I}}] - \mathbb{E}[\mathbf{Y}]\mathbb{E}[\widehat{\mathbf{I}}] = \beta \left(\mathbb{E}[\mathbf{T}\widehat{\mathbf{I}}] - \mathbb{E}[\mathbf{T}]\mathbb{E}[\widehat{\mathbf{I}}] \right) = \beta \text{Cov}(\mathbf{T}, \widehat{\mathbf{I}}),$$

we have $\dfrac{\text{Cov}(\mathbf{Y}, \widehat{\mathbf{I}})}{\text{Cov}(\mathbf{T}, \widehat{\mathbf{I}})} = \beta = \dfrac{\text{Cov}(\mathbf{Y}, \mathbf{I})}{\text{Cov}(\mathbf{T}, \mathbf{I})}$. Therefore, we have shown another example where the measurement $\widehat{\mathbf{I}}$ can serve as a drop-in replacement for the latent instrumental variable $\mathbf{I}$ for downstream causal inference tasks.